DALTON
FULL PAPER

$Re^{I}(CO)_3^+$ complexes with N∩O⁻ bidentate ligands

Rafal Czerwieniec,[a] Andrzej Kapturkiewicz,*[a] Romana Anulewicz-Ostrowska[b] and Jacek Nowacki[b]

[a] *Institute of Physical Chemistry, Polish Academy of Sciences, Kasprzaka 44/52, 01-224 Warsaw, Poland. E-mail: akaptur@ichf.edu.pl*
[b] *Department of Chemistry, Warsaw University, Pasteura 1, 02-093 Warsaw, Poland*

Received 25th April 2002, Accepted 19th July 2002
First published as an Advance Article on the web 23rd August 2002

Simple reactions between $Re(CO)_5Cl$ and 2-benzoxazol-2-ylphenol, 2-benzothiazol-2-ylphenol or 2-(1-methyl-1*H*-benzoimidazol-2-yl)phenol (performed in boiling toluene) lead to dimeric complexes of general formula $Re_2(CO)_6(N\cap O^-)_2$. The obtained dimeric species are quite stable in non-coordinating solvents, but in coordinating media (*e.g.*, pyridine – pyr) they undergo disscociative solvolysis to form monomeric derivatives of general formula $Re(CO)_3(N\cap O^-)$pyr. Molecular structures of both the dimeric and monomeric forms have been confirmed by means of X-ray measurements, electron impact mass spectrometry and IR spectroscopic investigations. UV-VIS absorption and emission properties of the newly synthesized $Re(CO)_3^+$ complexes have been investigated and briefly compared with those previously reported for their 8-oxyquinolinato analogues.

Introduction

In recent decades the chemistry and photophysics of d^6 transition metal complexes with various organic ligands have been the object of numerous investigations.[1] Particularly the properties of $Re(CO)_3^+$ carbonyl complexes have attracted much attention. The $Re(CO)_3^+$ core is known[2–5] to form stable luminescent complexes with N∩N bidentate neutral ligands (*e.g.*, 2,2′-bipyridine or 1,10-phenanthroline and their derivatives) yielding both neutral *fac*-$Re(CO)_3(N\cap N)X$ (where X = Cl^-, Br^-, I^-) and ionic complexes *fac*-$Re(CO)_3(N\cap N)L^+$ (where L = ligand axial to the N∩N plane). The photophysical and photochemical behavior of these species were shown to be governed by the relative energetic position and interplay of the closely lying excited states of different character: MLCT, LLCT or IL, and correlations with the structure of the complexes were found.[6] The studies on these $Re(CO)_3^+$ complexes have received additional momentum since they offer the opportunity to investigate some fundamental physical problems.[7] Such compounds have also proved to be useful in some biophysical studies[8] and have been utilized (or proposed) for versatile practical applications covering such fields as photocatalysis,[9,10] electrocatalysis[11,12] or luminescent (bio)molecular probes and labels.[13,14]

Apart from the neutral N∩N ligands the $Re(CO)_3^+$ core was also shown to form complexes with some anionic ligands, in particular with the N∩C⁻ bidentate benzo[*h*]quinoline (bzqH) and 2-phenylpyridine (ppyH) ligands,[15,16] which are structurally similar to the 2,2′-bipyridine or 1,10-phenanthroline derivatives. In the search for other neutral $Re(CO)_3^+$ complexes the reaction between $Re(CO)_5Cl$ and 8-hydroxyquinoline (HOX) was applied as a simple synthetic route to obtain a product with the proposed formula $Re(CO)_4(OX)$[17] (on the basis of the elemental analysis only) analogous to the $Re(CO)_4$(ppy) or $Re(CO)_4$(bzq) species.

$$Re(CO)_5Cl + HOX \longrightarrow Re(CO)_4(OX) + CO + HCl \quad (1)$$

However, more detailed analysis[18] (X-ray, EIMS and IR spectroscopic studies) revealed that the direct product of reaction (1) is the dimeric complex $Re_2(CO)_6(OX)_2$ (*cf.* Fig. 1):

$$2Re(CO)_5Cl + 2HOX \longrightarrow Re_2(CO)_6(OX)_2 + 4CO + 2HCl \quad (2)$$

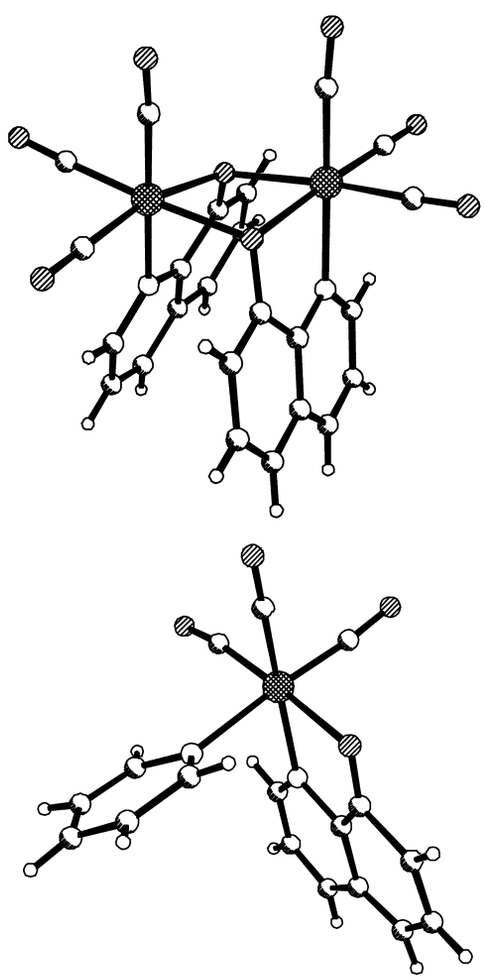

Fig. 1 ORTEP drawings of $Re_2(CO)_6(OX)_2$ (top) and $Re(CO)_3(OX)$-pyr (bottom) (data from ref. 18).

The dimeric $Re_2(CO)_6(OX)_2$ was found to be relatively stable in non-coordinating solvents but underwent (in high donicity media such as pyridine, *N*,*N*-dimethylformamide, acetonitrile

 DOI: 10.1039/b204020d

or dimethyl sufoxide) dissociative solvolysis yielding the monomeric species $Re(CO)_3(OX)solv$ (*cf.* Fig. 1):

$$Re_2(CO)_6(OX)_2 + 2solv \longrightarrow 2Re(CO)_3(OX)solv \quad (3)$$

In view of the above-mentioned findings it seemed to be reasonable to infer that other $N\cap O^-$ ligands with suitably located heteroaromatic N atoms and OH groups would form similar complexes. In order to confirm this hypothesis and to answer the question 'is the reaction pattern observed in the case of HOX (*i.e.*, the primary formation of a complex in the dimeric form) more common than monomer formation?', we decided to study the reactions of $Re(CO)_5Cl$ with the following agents: 2-benzoxazol-2-ylphenol, 2-benzothiazol-2-ylphenol and 2-(1-methyl-1*H*-benzoimidazol-2-yl)phenol along with the physicochemical properties of the eventual products. Here we present the preliminary results of our investigations.

Experimental

Materials

2-(1-Methyl-1*H*-benzoimidazol-2-yl)phenol (BIPH – synthesized as described in ref. 19) and commercially available 2-benzoxazol-2-ylphenol (BOPH – Aldrich) and 2-benzothiazol-2-ylphenol (BTPH – Lancaster), see Fig. 2, were used for reactions with $Re(CO)_5Cl$ (Strem Chemicals). Butyronitrile (BN – Merck, for synthesis) was triply distilled over $KMnO_4$ + K_2CO_3, P_2O_5, and CaH_2, successively. All other solvents used for our studies were of spectroscopic grade (Aldrich or Merck). Solutions for the emission measurements were deaerated by saturation with argon.

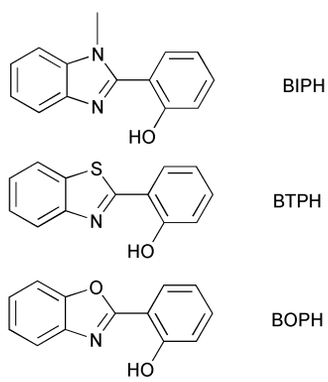

Fig. 2 Structural formulae of the studied ligands: 2-(1-methyl-1*H*-benzoimidazol-2-yl)phenol (BIPH), 2-benzothiazol-2-ylphenol (BTPH) and 2-benzoxazol-2-ylphenol (BOPH).

Syntheses

$Re_2(CO)_6(BOP)_2$, $Re_2(CO)_6(BTP)_2$ and $Re_2(CO)_6(BIP)_2$. These compounds were obtained (in almost quantitative yields) by reacting an equimolar suspension of $Re(CO)_5Cl$ and appropriate coordinating agent in refluxing toluene under argon for about 3 hours. After cooling to room temperature the dimeric complexes precipitated as fine yellowish or white (in the case of the latter complex) powders. The crude products were washed using dichloromethane (DCM) to remove the excess unreacted reagents. Elemental analysis: $Re_2(CO)_6(BOP)_2$ – found C, 40.03; H, 1.70; N, 2.84; $C_{32}H_{16}N_2O_{10}Re_2$ requires C, 40.00; H, 1.68; N, 2.92%. $Re_2(CO)_6(BTP)_2$ – found C, 38.42; H, 1.59; N, 2.63; S, 6.29; $C_{32}H_{16}N_2O_8Re_2S_2$ requires C, 38.70; H, 1.62; N, 2.82; S, 6.43%. $Re_2(CO)_6(BIP)_2$ – found C, 41.35; H, 2.11; N, 5.56; $C_{34}H_{22}N_4O_8Re_2$ requires C, 41.37; H, 2.25; N, 5.68%.

$Re(CO)_3(BOP)pyr$, $Re(CO)_3(BTP)pyr$ and $Re(CO)_3(BIP)pyr$. These compounds were obtained by dissolving $Re_2(CO)_6(BOP)_2$, $Re_2(CO)_6(BTP)_2$ or $Re_2(CO)_6(BIP)_2$ in pyridine (pyr), heating the solution under reflux until the dissociative solvolysis (*wide infra*) was complete followed by subsequent slow evaporation of the excess solvent. The crude products were recrystallized from hexane/DCM mixtures giving respectively bright yellow, yellow and white X-ray quality crystals. Elemental analysis: $Re(CO)_3(BOP)pyr$ – found C, 45.02; H, 2.21; N, 4.87; $C_{21}H_{13}N_2O_5Re$ requires C, 45.08; H, 2.34; N, 5.00%. $Re(CO)_3(BTP)pyr$ – found C, 43.73; H, 2.43; N, 4.72; S, 5.44; $C_{21}H_{13}N_2O_4ReS$ requires C, 43.82; H, 2.28; N, 4.87; S, 5.57%. $Re(CO)_3(BIP)pyr{\cdot}CH_2Cl_2$ (according to the X-ray results) – found C, 41.82; H, 2.93; N, 6.52; $C_{22}H_{16}N_2O_4Re{\cdot}CH_2Cl_2$ requires C, 42.01; H, 2.76; N, 6.39%.

Techniques

Electron impact mass spectra (EIMS) were recorded on an Intectra GmbH AMD 604 mass spectrometer. IR and UV-VIS absorption was measured by means of a Perkin-Elmer Spectrum 2000 FT-IR and Shimadzu UV 2401 PC spectrophotometers, respectively. Luminescence spectra (corrected for the spectral sensitivity of the instrument) were recorded using an Edinburgh Instruments FS900 steady-state fluorimeter. As a quantum yield standard a solution of quinine sulfate in 0.1 N H_2SO_4 ($\phi_o = 0.51$ [20]) was used. Low-temperature (77 K) luminescence spectra in butyronitrile and toluene glasses were recorded by means of a Jasny spectrofluorimeter.[21] Luminescence lifetime measurements have been performed using a home-built set-up[22] with the excitation provided by a MSG 350S nitrogen laser (LTB Lasertechnik Berlin) with a pulse duration of 0.6 ns (fwhm). The dispersed emission was detected using a RCA 1P28 photomultiplier connected to a Tektronix TDS420A digital scope. In all the cases studied the luminescence decays (analyzed by the single-curve method) were monoexponential on the microsecond scale of observation.

Crystallographic data regarding structures of monomeric $Re(CO)_3(BOP)pyr$ (**I**), $Re(CO)_3(BTP)pyr$ (**II**) and $Re(CO)_3(BIP)pyr$ (**III**) are collected in Table 1 together with refinement details. X-Ray measurements were performed on a Kuma KM4CCD κ-axis diffractometer with graphite-monochromated Mo-Kα radiation. The crystal was positioned at 62.25 mm from the KM4-CCD camera. 600 (**I**), 1000 (**II**) and 856 (**III**) frames were measured at 1° (**I**), 1.2° (**II**) and 1.4° (**III**) intervals with a counting time of 30 s (**I**), 15 s (**II**) and 25 s (**III**), correspondingly. The data were also corrected for Lorentz and polarization effects and numerical absorption correction was applied. Data reduction and analysis were carried out with the Kuma Diffraction (Wroclaw) programs. The structures were solved by direct methods[23] and refined using the SHELXL computer program.[24] The refinement was based on F^2 for all reflections except those with very negative F^2. Weighted R factors wR and all goodness-of-fit S values are based on F^2. Conventional R factors are based on F with F set to zero for negative F^2. The $F_o^2 > 2\sigma(F_o^2)$ criterion was used only for calculating R factors and is not relevant to the choice of reflections for the refinement. The R factors based on F^2 are about twice as large as those based on F. All hydrogen atoms were placed in calculated positions and their thermal parameters were refined isotropically. Scattering factors were taken from Tables 6.1.1.4 and 4.2.4.2 of ref. 25.

CCDC reference numbers 184541 (**I**), 184542 (**II**) and 184543 (**III**).

See http://www.rsc.org/suppdata/dt/b2/b204020d/ for crystallographic data in CIF or other electronic format.

Results and discussion

Molecular structures

Despite the fact that the results from the elemental analyses correspond quite well to the assumed molecular formulae of

Table 1 Crystal data and structure refinement for $Re(CO)_3L(pyr)$ molecules

	$Re(CO)_3(BIP)(pyr)$	$Re(CO)_3(BOP)(pyr)$	$Re(CO)_3(BTP)(pyr)$
Chemical formula	$C_{22}H_{16}N_3O_4Re{\cdot}CH_2Cl_2$	$C_{21}H_{13}N_2O_5Re$	$C_{21}H_{13}N_2O_4ReS$
Formula weight	657.50	559.53	575.59
Crystal systems	Monoclinic	Monoclinic	Triclinic
a/Å	14.878(3)	9.517(2)	8.749(2)
b/Å	15.228(3)	15.171(3)	10.111(2)
c/Å	11.207(2)	13.697(3)	13.891(3)
α/°			73.11 (3)
β/°	107.96(3)	104.77(3)	74.65(3)
γ/°			67.79(3)
U/Å	2415.4(8)	1912.3(7)	1071.8(4)
T/K	293(2)	293(2)	293(2)
Space group	*P*2(1)/*c*	*P*2(1)/*c*	$P\bar{1}$
Z	4	4	2
μ/nm^{-1}	5.286	6.391	5.79
R indices (all data)	0.0828; $wR(F^2) = 0.0915$	0.0660; $wR(F^2) = 0.1732$	0.0623; $wR(F^2) = 0.1461$
Final *R* indices [$I > 2\sigma(I)$]	0.0461; $wR(F^2) = 0.0795$	0.0601; $wR(F^2) = 0.1577$	0.0493; $wR(F^2) = 0.1230$

Table 2 Lengths of the selected bonds in the studied $Re(CO)_3(N{\cap}O^-)pyr$ complexes[a]

	$Re(CO)_3(BIP)pyr$	$Re(CO)_3(BTP)pyr$	$Re(CO)_3(BOP)pyr$	$Re(CO)_3(OX)pyr$[b]
$Re–N_{pyr}$	2.230(8)	2.186(6)	2.203(10)	2.204(4)
$Re–N_{chel}$	2.151(7)	2.177(6)	2.198(10)	2.162(3)
$Re–O_{chel}$	2.130(7)	2.093(5)	2.101(9)	2.099(3)
$C–O_{chel}$	1.308(11)	1.311(9)	1.280(14)	1.321(5)
C–Re	1.84(2), 1.905(13), 1.919(12)	1.911(9), 1.916(8), 1.918(9)	1.863(12), 1.88(2), 1.91(2)	1.913(5), 1.917(5), 1.917(4)
C–O	1.203(14), 1.145(12), 1.139(12)	1.131(11), 1.124(10), 1.121(10)	1.16(2), 1.16(2), 1.13(2)	1.134(6), 1.140(6), 1.151(5)

[a] Distances between $Re–N_{pyr}$ (Re and pyridine N atoms), $Re–N_{chel}$ (Re and the chelate N atoms), $Re–O_{chel}$ (Re and the chelate O atoms), $C–O_{chel}$ (phenolic group in the chelate subunit), C–Re (between Re and C atoms of the carbonyl groups) and C–O (C and O atoms within the carbonyl groups), respectively. [b] Data for $Re(CO)_3(OX)pyr$ complex from ref. 18.

the compounds under study, they have been confirmed by more detailed structural investigation. Due to the fact that from solutions of the direct products of the reactions between $Re(CO)_5Cl$ and BOPH, BTPH or BIPH in non-coordinating solvents only extremely fine powders precipitated and also due to the necessity of keeping the samples away from coordinating media we were unable to obtain X-ray quality crystals of the presumably dimeric species. On the other hand, for the second set of investigated compounds, presumably monomeric ones, this was possible. The obtained X-ray results are in nice agreement with the expected monomeric character of these species. Despite the fact that the *R* factors indicate low quality for the studied crystals the obtained crystallographic data give a good insight into the molecular structures.

The ORTEP[26] schemes of the $Re(CO)_3(BIP)pyr$, $Re_2(CO)_3(BOP)pyr$ and $Re(CO)_3(BTP)pyr$ derivatives are presented in Fig. 3 and the relevant $Re–N_{pyr}$ and $Re–N_{chel}$ bond lengths are collected in Table 2. The data indicate approximately the same affinity of the axial pyridine ligand for the $Re(CO)_3(N{\cap}O^-)$ core in all the complexes under study. The comparison of lengths of the bonds between Re and N_{chel} (from the $N{\cap}O^-$ ligand) reveals a similar affinity of the $N{\cap}O^-$ ligands for the $Re(CO)_3^+$ core within the $Re(CO)_3(N{\cap}O^-)$ subunits. Moreover, in each complex, N_{chel} is more strongly bound to the $Re(CO)_3^+$ core than the pyridine N_{pyr} atom. On the basis of the bond lengths the covalent character of the $Re–N_{pyr}$ and $Re–N_{chel}$ bonds may also be proposed (*cf.* refs. 27–29). On the other hand, bond lengths between Re and O_{chel} (being in the range 2.093–2.130 Å) or C and O_{chel} (within the $N{\cap}O^-$ chelate, being in the range 1.28–1.32 Å) support the ionic character of the O_{chel} atom and correspondingly the enol character of the ligands. As can be expected for a pseudo-octahedral structure the three carbonyl groups in the $Re(CO)_3(N{\cap}O^-)pyr$ complexes are characterised by different Re–C and C–O distances. It is nicely reflected in the IR-absorption spectra, particularly in the carbonyl stretching vibrations (ν_{CO}) spectral region where three distinct ν_{CO} bands can be observed (*cf.* Fig. 4). This behavior is characteristic for monomeric pseudo-octahedral *fac*-$Re(CO)_3^+$ complexes.[30–32]

Contrary to this, the IR spectra recorded for the complexes from the first group (primary products of the reactions between $Re(CO)_5Cl$ and $N{\cap}OH$ ligands) are distinctly different (*cf.* Fig. 4). Similar to what was found previously for the $Re_2(CO)_6(OX)_2$ complex one can clearly observe two close bands at ≈ 2015–2030 cm^{-1} and a group of broad, merged bands around 1900 cm^{-1}. The observed splitting (clearly seen in the region 2015–2030 cm^{-1}) may be attributed to the dimeric structure of the studied species similar to the case of the $Re_2(CO)_6(OX)_2$ complex. It should be noted, however, that the IR data for the complexes presently under study are less informative when compared to those for $Re_2(CO)_6(OX)_2$, because of the much more pronounced band overlapping in the region ≈1900 cm^{-1}.

Additional information about the structures of the investigated complexes can be obtained from the mass spectrometry investigations. Similar to what was found for the $Re_2(CO)_6(OX)_2$ complex, EIMS spectra (*cf.* Fig. 5) express all the features characteristic of dimeric structures. It has been found that the most intense peaks correspond to the mass/charge ratios characteristic of the $Re(N{\cap}O^-)^+$ ions, but the presence of $Re_2(CO)_n(N{\cap}O^-)_2^+$ (with n = 0–6) as well as $Re(CO)_m(N{\cap}O^-)^+$ (with m = 1–3) is clearly seen. For all of the detected ions one can find a characteristic set of signals resulting from the natural abundance (37 and 63%, respectively) of ^{185}Re and ^{187}Re isotopes. The results of the EIMS investigations, *i.e.*, apparently various ratios of the peak intensities corresponding to the $Re(CO)_m(N{\cap}O^-)^+$ and $Re_2(CO)_n(N{\cap}O^-)_2^+$ fragmentation ions, suggest a different stability for the dimeric species.

In view of the above described IR and EIMS results, the dimeric nature of the products obtained directly from the reactions of $Re(CO)_5Cl$ with the $N{\cap}OH$ chelating agents seems to be well proved. One can also speculate that the $Re(CO)_3(N{\cap}O^-)$ subunits of the dimeric species are merged *via* O_{chel} atoms with a four-membered ring: $Re–O_{chel}–Re–O_{chel}$ formed similarly to $Re_2(CO)_6(OX)_2$.

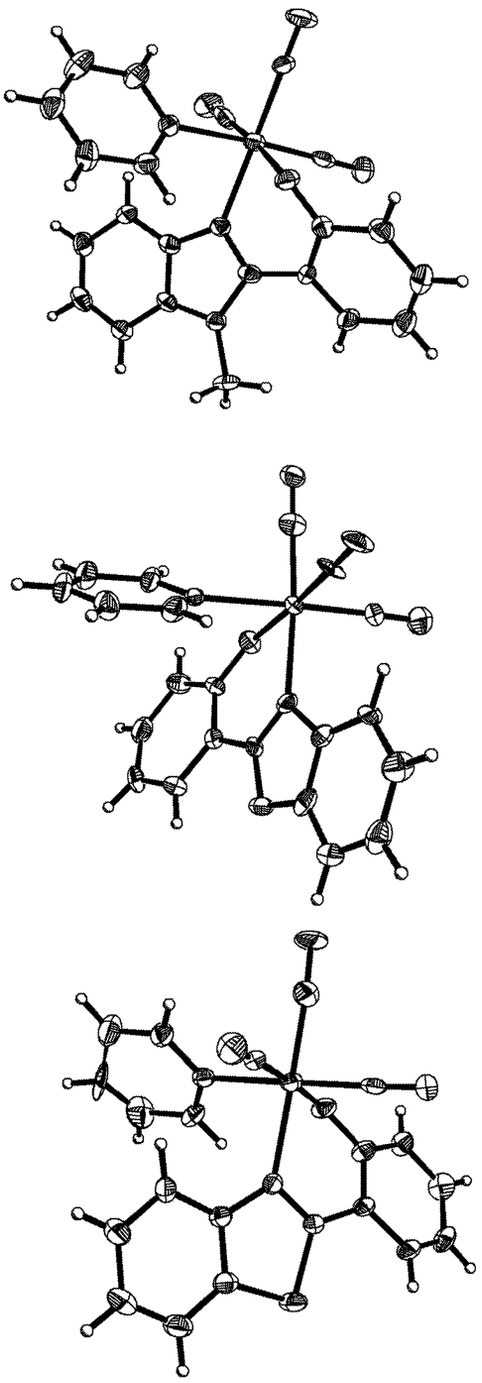

Fig. 3 ORTEP drawings of $Re(CO)_3(BIP)pyr$ (top), $Re(CO)_3(BOP)$-pyr (center) and $Re(CO)_3(BTP)pyr$ (bottom) showing 30% probability ellipsoids.

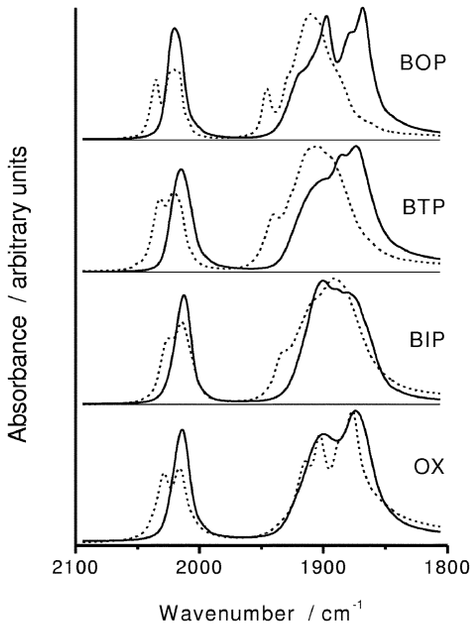

Fig. 4 IR spectra (the carbonyl stretching region) of dimeric $Re_2(CO)_6(N\cap O^-)_2$ (dashed lines) and monomeric $Re_2(CO)_3(N\cap O^-)pyr$ (solid lines) in KBr pellets. $N\cap O^-$ = BOP, BTP, BIP, OX.[18]

UV-VIS absorption spectra

The solubility of the studied complexes in organic solvents varies significantly. Generally, the dimeric species are much less soluble in organic solvents than the monomeric ones with a clear preference towards non-polar solvents in the case of the former. The UV-VIS absorption spectra of $Re_2(CO)_6(BOP)_2$ and $Re_2(CO)_6(BTP)_2$ in non-coordinating media (*e.g.*, DCM) look very similar to each other. The only difference is the red shift of the respective absorption bands of $Re_2(CO)_6(BTP)_2$ as compared to its $Re_2(CO)_6(BOP)_2$ analogue with the spectral pattern preserved (*cf.* Fig. 6). The spectra are characterized by the presence of the low-energy absorption band at 350 or 370 nm (for $Re_2(CO)_6(BOP)_2$ and $Re_2(CO)_6(BTP)_2$, respectively) partially obscured by the next band with a distinctly higher molecular extinction coefficient with absorption maxima at 295 nm or 315 nm, respectively. The spectra of the relevant monomeric $Re(CO)_3(BOP)pyr$ and $Re(CO)_3(BTP)pyr$ also comprise a strong absorption below 350 nm with the positions of the second bands nearly unchanged when compared to the parent dimeric forms. The lowest-energy bands, however, occur at much lower wavelengths (410 and 430 nm, respectively) than in the spectra of $Re_2(CO)_6(BOP)_2$ and $Re_2(CO)_6(BTP)_2$. The assignment of the higher energy part of the spectra of all four compounds may be related to the electronic transitions in the $N\cap O^-$ ligands[33,34] somewhat distorted by coordination of the heavy metal core. On the other hand, the profound dependence of the spectral position of the lowest energy bands on the structure of the complex, particularly on the ligand environment of the $Re(CO)_3^+$ core, seems to suggest metal-to-ligand charge-transfer (MLCT) character (spin allowed $S_0 \longrightarrow {}^1$MLCT transition). Solvent induced changes in the UV-VIS spectra (expressed in terms of different sensitivity of the absorption maxima positions to solvent polarity) agree quite well with the preasumably dominant MLCT or IL character of the lowest and energetically higher bands, respectively. Note, that the axial ligand pyr in the $Re(CO)_3(N\cap O^-)pyr$ molecules is most probably replaced by solv in strongly coordinating media like amides or nitriles.

The UV-VIS absorption spectrum of $Re_2(CO)_6(BIP)_2$ is somewhat different. The observed absorption band at 285 nm (related to the intra-ligand transition in BIP[35]) most probably overlays the expected $S_0 \longrightarrow {}^1$MLCT transition. On the other hand, the UV-VIS spectral behavior of the $Re(CO)_3(BIP)pyr$ complex (with the presumably $S_0 \longrightarrow {}^1$MLCT band localized at 355 nm) is more or less similar to that found for $Re(CO)_3(BOP)pyr$ or $Re(CO)_3(BTP)pyr$.

Distinct changes in the UV-VIS spectra of the dimeric complexes are observed in strongly coordinating solvents (*e.g.*, *N*-methylpyrrolidone) where bathochromic shifts in the position of the $S_0 \longrightarrow {}^1$MLCT transitions to that characteristic for the monomeric species are clearly seen (*cf.* Fig. 7). The interactions with the solvent medium lead to profound changes in the UV-VIS properties probably due to the solute structural rearrangement. Similarly as was previously[18] found for the $Re_2(CO)_6(OX)_2$ and $Re(CO)_3(OX)pyr$ pair the observed UV-VIS spectral behavior may be attributed to the dissociative solvolysis of the $Re_2(CO)_6(N\cap O^-)_2$ species:

$$Re_2(CO)_6(N\cap O^-)_2 + 2solv \longrightarrow 2Re(CO)_3(N\cap O^-)solv \quad (4)$$

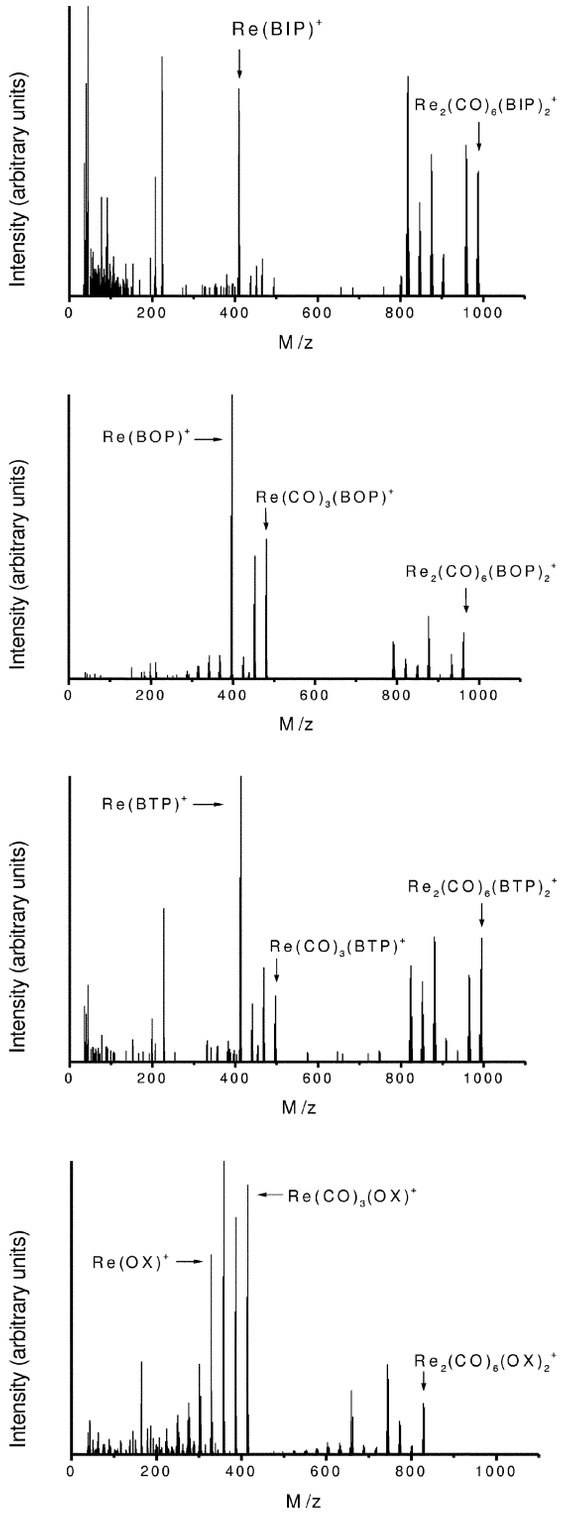

Fig. 5 EIMS spectra of the $Re_2(CO)_6(N\cap O^-)_2$ molecules; $Re_2(CO)_6(BIP)_2$, $Re_2(CO)_6(BOP)_2$, $Re_2(CO)_6(BTP)_2$, $Re_2(CO)_6(OX)_2$ (from top to bottom).

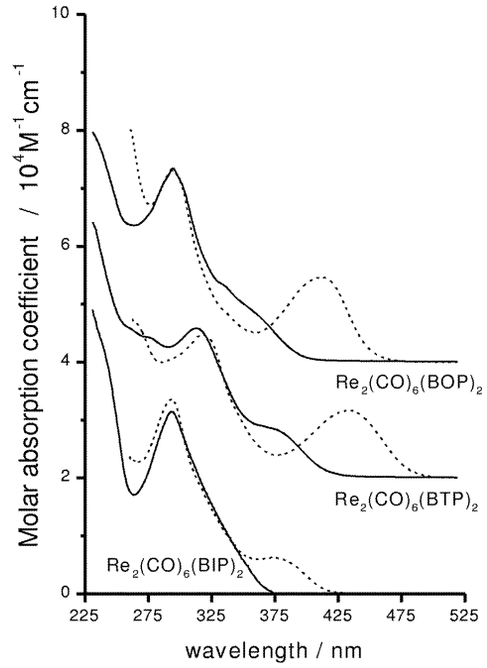

Fig. 6 UV-VIS absorption spectra of $Re_2(CO)_6(BOP)_2$, $Re_2(CO)_6(BTP)_2$ and $Re_2(CO)_6(BIP)_2$ in *N*-methylpyrrolidone (dashed lines) and in dichloromethane (solid lines) solutions. The spectra of $Re_2(CO)_6(BTP)_2$ and $Re_2(CO)_6(BOP)_2$ are shifted along the *y*-axis (by factors 2×10^4 and 4×10^4 M^{-1} cm^{-1}, respectively).

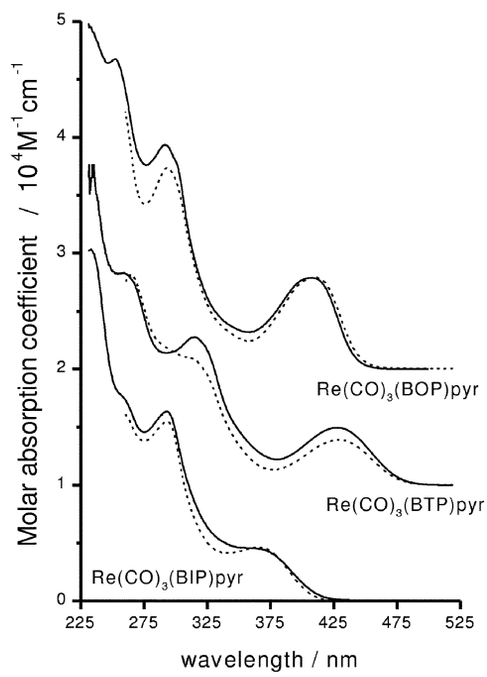

Fig. 7 UV-VIS absorption spectra of $Re(CO)_3(BOP)pyr$, $Re(CO)_3(BTP)pyr$ and $Re(CO)_3(BIP)pyr$ in *N*-methylpyrrolidone (dashed lines) and in dichloromethane (solid lines) solutions. The spectra of $Re(CO)_3(BTP)pyr$ and $Re(CO)_3(BOP)pyr$ are shifted along the *y*-axis (by factors 1×10^4 and 2×10^4 M^{-1} cm^{-1}, respectively).

It should be noted, however, that the solvolysis process is relatively slow in the case of the presently studied complexes, much slower than for $Re_2(CO)_2(OX)_2$. The difference is especially large for the $Re_2(CO)_6(BTP)_2$ and $Re_2(CO)_6(BIP)_2$ complexes where hours or days are necessary for conversion of $Re_2(CO)_6(N\cap O^-)_2$ into $Re(CO)_3(N\cap O^-)$solv. This indicates relatively high stability of these $Re_2(CO)_6(N\cap O^-)_2$ dimers in accordance with the EIMS results – relatively high peak intensities of the $Re_2(CO)_n(N\cap O^-)_2^+$ ions as compared to other ionization fragments (*cf.* Fig. 5).

The intrinsic differences in the UV-VIS absorption spectra between the monomeric and dimeric complexes may be utilized to monitor the presence of each form in solution. In particular the absorbance above 400 nm may serve as a fingerprint of the monomeric forms. A typical example of the time evolution of the UV-VIS absorption spectra for the $Re_2(CO)_6(BOP)_2$–pyridine system is presented in Fig. 8.

This has allowed us to observe the temporal changes in the composition of the solutions after dissolving $Re_2(CO)_6(N\cap O^-)_2$ in a coordinating medium (pyridine or pyridine/DCM mixtures) and thus to investigate the kinetics of the dissociative

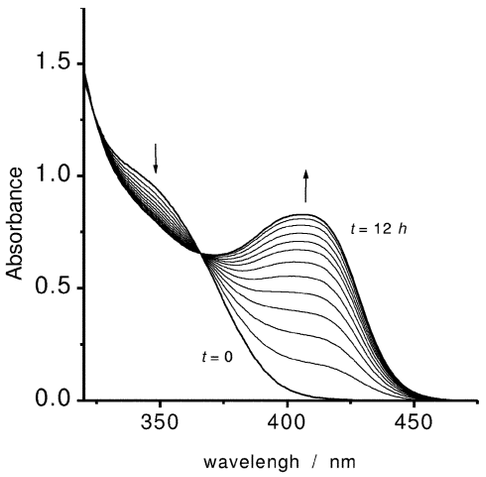

Fig. 8 Time evolution of UV-VIS absorption spectra (recorded at 1 h intervals) for 10^{-4} M solutions of $Re_2(CO)_6(BOP)_2$ in DCM after addition of pyridine (C_{solv} = 0.83 M).

solvolysis reactions. Kinetic studies (for details see ref. 18) have established that dissociative solvolysis is a first order reaction with respect to each reactant, similar to what was found for the $Re_2(CO)_6(OX)_2$–pyridine system[18] (with k_{solv} = 6.4 × 10^{-3} M^{-1} s^{-1} in DCM solutions). Spectroscopic studies also indicate a complete chemical rearrangement of $Re_2(CO)_6(N\cap O^-)_2$ into $Re(CO)_3(N\cap O^-)$solv that allows for simple kinetic analysis if a high excess of the solvolysing agent (with concentration C_{solv}) is applied (pseudo-zero-order conditions). In such a case the absorbance $A(t)$, measured at a given wavelength in the lowest absorption band of the monomeric form, is a simple function of time t:

$$A(t) = A(\infty) \times [1 - \exp(-k_{solv}C_{solv}t)] \qquad (5)$$

where k_{solv} and $A(\infty)$ are the solvolysis rate constant and the equilibrated solution absorbance. The second order solvolysis rate constant k_{solv} = 5.7 × 10^{-5} M^{-1} s^{-1} for $Re_2(CO)_6(BOP)_2$ has been obtained in DCM/pyridine mixtures. Solvolyses of $Re_2(CO)_6(BTP)_2$ and $Re_2(CO)_6(BIP)_2$ are still slower processes with k_{solv} (in pure pyridine solutions) being 1.8 × 10^{-6} and 5.5 × 10^{-7} M^{-1} s^{-1}, respectively. Noteworthy, the solvolysis rates seem to be correlated with the relative stabilitities of the $Re_2(CO)_6(N\cap O^-)_2$ dimers as suggested by the EIMS results (*vide supra*).

Luminescence properties

All the monomeric species under study show relatively intense luminescence in various solutions, *e.g.*, emission quantum efficiencies of 0.032, 0.025 and 0.021 have been found in DCM for the $Re(CO)_3$(BOP)pyr, $Re(CO)_3$(BTP)pyr and $Re(CO)_3$(BIP)pyr complexes, respectively. The room temperature emission spectra are broad and structureless (*cf.* Fig. 9–11). The lifetimes of a few microseconds indicate a considerable contribution of the ^{3}MLCT character to the emitting excited state. The luminescence spectra recorded at 77 K look different, exhibiting structured and considerably blue shifted bands with a vibronic progression of *ca.* 1500 cm^{-1}. Moreover, the emission lifetimes of the $Re(CO)_3(N\cap O^-)$pyr species are about ten times longer as compared with the room temperature values. Both findings point to a different origin for the monomeric species emissions in both temperature regimes. As the vibronic structure of the 77 K luminescence resembles the shape of relevant free ligands phosphorescence[33,36,37] we assign the 77 K emission as originating from the locally excited state mostly localized within the ligand (IL).

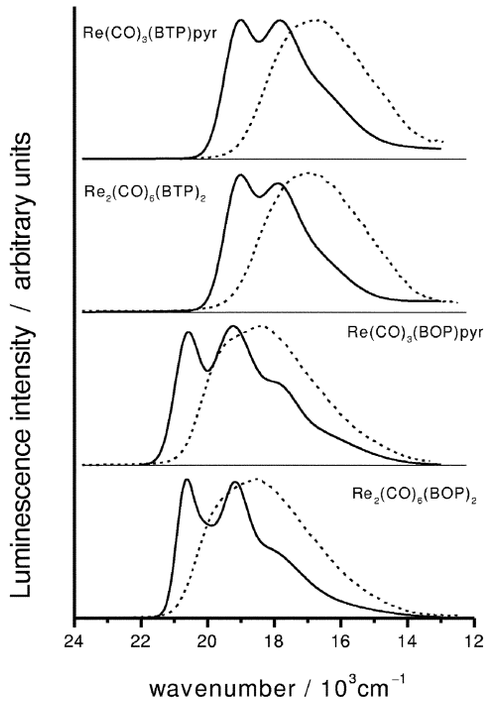

Fig. 9 Luminescence spectra of the dimeric $Re_2(CO)_6(BOP)_2$ and $Re_2(CO)_6(BTP)_2$ and monomeric $Re(CO)_3$(BOP)pyr and $Re(CO)_3$(BTP)pyr complexes in butyronitrile solutions at room temperature (dashed lines) and in butyronitrile glasses at 77 K (solid lines).

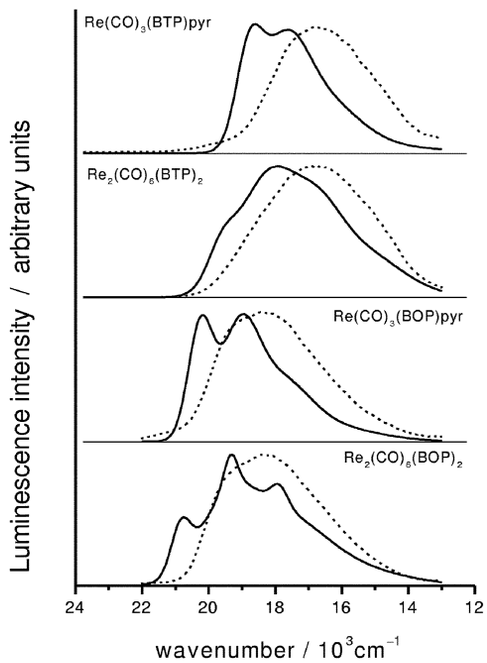

Fig. 10 Luminescence spectra of the dimeric $Re_2(CO)_6(BOP)_2$ and $Re_2(CO)_6(BTP)_2$ and monomeric $Re(CO)_3$(BOP)pyr and $Re(CO)_3$(BTP)pyr complexes in toluene solutions at room temperature (dashed lines) and in toluene glasses at 77 K (solid lines).

Room temperature spectral properties of the monomeric complexes are only weakly dependent on the solvent used, particularly its polarity. Thus, the variation of the character of the luminescent state on lowering the temperature is not caused by the differences of the solvent polarity, but most probably corresponds to the change of medium rigidity upon freezing below the liquid–glass transition temperature. Similar effects, *i.e.*, the altering of the emission character from the MLCT in solutions to IL in rigid media, have already been observed for some other $Re(CO)_3^+$ organometallic complexes.[38,39] Such a variation of emitting properties requires the coexistance of two

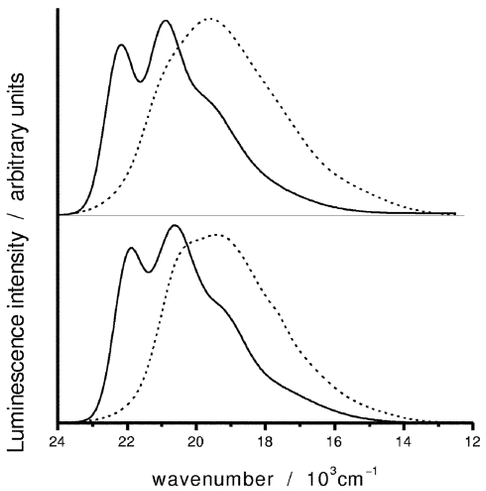

Fig. 11 Luminescence spectra of $Re(CO)_3(BIP)pyr$ in butyronitrile (top) and toluene (bottom) solutions at room temperature (dashed lines) and in 77 K glasses (solid lines).

close in energy excited states of different types (MLCT and IL, respectively) and arises from the different sensitivity of the energy levels of these states to the inner- and outer-reorganization of the solute/solvent system. At low temperatures the high viscosity of the glass hinders the solute/environment relaxation.

The dimeric $Re_2(CO)_6(BOP)_2$ and $Re_2(CO)_6(BTP)_2$ complexes are also luminescent at room temperature but with quantum efficiencies lower than those found for the corresponding monomeric species (*e.g.*, values of 0.005 and 0.014, respectively, have been found in DCM solutions). The shape and spectral position of the observed emission bands are similar to the phosphorescence of relevant monomeric species. On the other hand we were unable to detect any emission from the $Re_2(CO)_6(BIP)_2$ molecule (even at 77 K).

The 77 K luminescence of the dimeric complexes in BN glasses prepared by freezing solutions (after the time necessary for the solvolysis reaction to be completed) are identical with the BN-glass spectra of the $Re(CO)_3(BOP)pyr$, $Re(CO)_3(BTP)$-pyr or $Re(CO)_3(BIP)pyr$ monomers. This indicates that the same emitting species, most probably $Re(CO)_3(N\cap O^-)BN$, are present in the BN solutions of both monomeric and dimeric complexes, suggesting the relatively labile character of the secondary ligand *e.g.*, pyridine.

The spectra of $Re_2(CO)_6(BOP)_2$ and $Re_2(CO)_6(BTP)_2$ in toluene glass at 77 K (non-coordinating medium) show vibronic structure with the pattern differing from that of the relevant monomeric $Re(CO)_3(BOP)pyr$ and $Re(CO)_3(BTP)pyr$. Obviously, in toluene solutions the dimeric complexes remain undissociated contrary to that in BN. The observed differences in shape of the emission bands, with apparently dominant ^{3}IL character, may be due to interactions between both π-systems (BOP or BTP ligands, correspondingly) present in the dimeric molecules. To discuss this aspect, data concerning their mutual orientation inside the dimeric complexes would be useful. However, due to problems with obtaining suitable crystals of $Re_2(CO)_6(BOP)_2$, $Re_2(CO)_6(BTP)_2$ and $Re_2(CO)_6(BIP)_2$ as mentioned above, the relevant structural information is not presently available.

Concluding remarks

The applied synthetic method yields new $Re(CO)_3^+$ complexes: monomeric ones of general formula $Re(CO)_3(N\cap O^-)solv$ (with structures confirmed by means of X-ray measurements) and dimers $Re_2(CO)_6(N\cap O^-)_2$ (with structures suggested by IR as well as EIMS studies). UV-VIS absorption investigations indicate that the dimeric complexes $Re_2(CO)_6(N\cap O^-)_2$ undergo dissociative solvolysis in a wide range of coordinating solvents. The solvolysis rates (with pyridine as the solvolysing agent) have been found to correlate with the relative stability (in the gas phase) of the dimeric $Re_2(CO)_6(N\cap O^-)_2$ species.

The monomeric $Re(CO)_3(N\cap O^-)pyr$ and dimeric $Re_2(CO)_6$-$(N\cap O^-)_2$ complexes exhibit different (particularly in the region of the spin allowed $S_0 \longrightarrow {}^1$MLCT transition) UV-VIS absorption spectra. The observed bathochromic shifts of the $S_0 \longrightarrow {}^1$MLCT band positions may probably be attributed to the better electron donating ability of the $Re(CO)_3pyr^+$ fragment (in the monomeric forms) as compared to $Re(CO)_3^+$ alone (in the dimeric complexes), which seems understandable. On the other hand the positions of the $S_0 \longrightarrow {}^1$MLCT bands indicate that the electron affinity of the chelating $N\cap O^-$ ligands increases in the order: $BTP^- > BOP^- > BIP^-$. Dimeric and monomeric complexes with BOP and BTP as the $N\cap O^-$ ligands are emissive at room temperature as well as at 77 K in contrast to the complexes with the BIP ligand where only the monomeric forms $Re(CO)_3(BIP)solv$ were found to show luminescence. Emission lifetime measurements point to the phosphorescent character of the luminescence. At liquid nitrogen temperature the emitting complexes exhibit structured luminescence (with band progression of *ca.* 1500 cm^{-1}) suggesting that the relevant excited states are completely localized within the chelating $N\cap O^-$ ligand. Room temperature emission bands have hardly any structure, which indicates that the emitting states have MLCT, or rather mixed IL/MLCT character. Moreover, the fact that the dimeric and monomeric species have nearly the same emission spectra suggests only weak electronic interactions between the $Re(CO)_3(N\cap O^-)$ subunits in the $Re_2(CO)_6$-$(N\cap O^-)_2$ molecules.

The obtained results indicate that the physicochemical behavior of the studied complexes is very similar to that found previously for the $Re(CO)_3(OX)pyr$ and $Re_2(CO)_6(OX)_2$ pair. Especially the fact that the studied $N\cap O^-$ chelates tend to form dimeric and monomeric species may suggest that it is a general rule for ligands of this type. Unfortunately lack of crystallographic data for the dimeric forms of the studied complexes does not allow for more detailed comparison of their structures. In view of the luminescence studies one can expect somewhat different (as compared to the $Re_2(CO)_6(OX)_2$ complex) arrangement of the $Re(CO)_3(N\cap O^-)$ subunits in the $Re_2(CO)_6(N\cap O^-)_2$ molecules. More detailed discussion of this structural aspect of $Re(CO)_3^+$ chemistry will be possible when appropriate data become available.

Acknowledgements

This work was partly sponsored by the Grant 7T09A11620 from the Committee of Scientific Research.

References

1 A. Vogler and H. Kunkely, *Coord. Chem. Rev.*, 2000, **200–202**, 991.
2 A. Juris, V. Balzani, F. Barigelletti, S. Campagna, P. Belser and A. von Zalewsky, *Coord. Chem. Rev.*, 1988, **84**, 85.
3 V. Balzani, A. Juris, M. Venturi, S. Campagna and S. Serroni, *Chem. Rev.*, 1996, **96**, 759.
4 D. R. Striplin and G. A. Crosby, *Coord. Chem. Rev.*, 2001, **211**, 136.
5 G. F. Strouse and H. U. Güdel, *Inorg. Chem.*, 1995, **34**, 5578.
6 D. J. Stuffkens and A. Vlček, Jr, *Coord. Chem. Rev.*, 1998, **177**, 127.
7 J. V. Caspar and T. J. Meyer, *J. Phys. Chem.*, 1983, **87**, 952.
8 W. B. Connick, A. J. Di Bilio, M. G. Hill, J. R. Winkler and H. B. Gray, *Inorg. Chim. Acta*, 1995, **240**, 169.
9 Y. Wang, B. T. Hauser, M. M. Rooney, R. D. Burton and K. S. Schanze, *J. Am. Chem. Soc.*, 1993, **115**, 5075.
10 V. W.-W. Yam, V. C.-Y. Lau and L.-X. Wu, *J. Chem. Soc., Dalton Trans.*, 1998, 1461.
11 M. Bakir and J. A. M. McKenzie, *J. Electroanal. Chem.*, 1997, **425**, 61.
12 F. P. A. Johnson, M. W. George, F. Hartl and J. J. Turner, *Organometallics*, 1996, **15**, 3374.

13 K. K.-W. Lo, D. C.-M. Ng, W.-K. Hui and K.-K. Cheung, *J. Chem. Soc. Dalton Trans.*, 2001, 2634.
14 K. K.-W. Lo, W.-K. Hui, D. C.-M. Ng and K.-K. Cheung, *Inorg. Chem.*, 2002, **41**, 40.
15 F. W. M. Vanhelmont, M. V. Rajasekharan, H. U. Güdel, S. C. Capelli, J. Hauser and H.-B. Bürgi, *J. Chem. Soc., Dalton Trans.*, 1998, 2893.
16 P. Spellane, R. J. Watts and A. Vogler, *Inorg. Chem.*, 1993, **32**, 5633.
17 H. Kunkely and A. Vogler, *Inorg. Chem. Commun.*, 1998, **1**, 398.
18 R. Czerwieniec, A. Kapturkiewicz, R. Anulewicz-Ostrowska and J. Nowacki, *J. Chem. Soc., Dalton Trans.*, 2001, 2756.
19 O. Fischer, *Chem. Ber.*, 1892, **25**, 2838.
20 R. A. Velapoldi, *NBS Spec. Publ. (US)*, 1972, **378**, 231.
21 J. Jasny, *J. Lumin.*, 1978, **17**, 143.
22 J. Karpiuk and Z. R. Grabowski, *Chem. Phys. Lett.*, 1989, **160**, 451.
23 G. M. Sheldrick, *Acta Crystallogr., Sect. A*, 1990, **46**, 467.
24 G. M. Sheldrick, SHELXL93, Program for Refinement of Crystal Structures, University of Göttingen, Göttingen 1993.
25 *International Tables for X-ray Crystallography*, Kynoch Press, Birmingham, 1974, vol. IV.
26 C. K. Johnson, ORTEP, Report ORNL-5138, Oak Ridge National Laboratory, Oak Ridge, TN, 1976.
27 R. Ballardini, G. Varani, M. T. Indelli and F. Scandola, *Inorg. Chem.*, 1986, **25**, 3858.
28 D. Donges, J. K. Nagle and H. Yersin, *J. Lumin.*, 1997, **72–74**, 658.
29 D. Donges, J. K. Nagle and H. Yersin, *Inorg. Chem.*, 1997, **36**, 3040.
30 G. J. Stor, F. Hartl, J. W. M. van Outersterp and D. J. Stufkens, *Organometallics*, 1985, **14**, 1115.
31 H. Hartmann, T. Schering, J. Fiedler and W. Kaim, *J. Organomet. Chem.*, 2000, **604**, 267.
32 M. K. Itokazu, A. S. Polo, D. L. A. de Faria, C. A. Bignozzi and N. Y. M. Iha, *Inorg. Chim. Acta*, 2001, **313**, 149.
33 W. Al-Soufi, K. H. Grellmann and B. Nickel, *J. Phys. Chem.*, 1991, **95**, 10503.
34 R. S. Becker, C. Lenoble and A. Zein, *J. Phys. Chem.*, 1987, **91**, 3509.
35 M. F. Rodríguez-Prieto, J. C. Penedo and M. Mosquera, *J. Chem. Soc., Faraday Trans.*, 1988, **94**, 2775.
36 M. F. Rodríguez-Prieto, B. Nickel, K. H. Grellmann and A. Mordzinski, *Chem. Phys. Lett.*, 1988, **146**, 387.
37 P. Chou, S. L. Studer and M. L. Martinez, *Chem. Phys. Lett.*, 1991, **178**, 393.
38 A. P. Zipp, L. Sacksteder, J. Streich, A. Cook, J. N. Demas and B. A. DeGraff, *Inorg. Chem.*, 1993, **32**, 5629.
39 W. Xue, M. C. Chan, Z. Su, K. Cheung, S. Liu and C. Che, *Organometallics.*, 1998, **17**, 1622.